2023 19th International Conference on Distributed Computing in Smart Systems and the Internet of Things (DCOSS-IoT)

2023 19th International Conference on Distributed Computing in Smart Systems and the Internet of Things (DCOSS-IoT) | 979-8-3503-4649-7/23/$31.00 ©2023 IEEE | DOI: 10.1109/DCOSS-IOT58021.2023.00075

Empirically Investigating the Impact of Antenna Polarization and Modulation Parameters on Subsoil Communication Range in LoRa Networks

1st Nhan D.T. Nguyen
Pervasive Group
University of Twente
Enschede, The Netherlands
d.t.n.nguyen@utwente.nl

2nd Duc V. Le
Pervasive Group
University of Twente
Enschede, The Netherlands
v.d.le@utwente.nl

3rd Paul J.M. Havinga
Pervasive Group
University of Twente
Enschede, The Netherlands
p.j.m.havinga@utwente.nl

***Abstract*—The Long Range (LoRa) network has been widely acknowledged for its efficiency and reliability in terrestrial sensing applications. However, building a robust LoRa network in the subsoil environment, which presents challenges for radio communication, remains challenging. This study evaluates the impact of antenna polarization and LoRa modulation parameters, such as bandwidth and spreading factor, on subsoil communication ranges. Based on the results of our experiments, we propose practical LoRa network configurations for the seamless transmission of subsoil sensory data to the surface.**

***Index Terms*—subsoil communication, LoRa, underground sensing and monitoring, underground sensor network**

I. Introduction

Effective monitoring and sensing of the subsoil layer offer numerous benefits for various applications related to the subsoil, including agriculture, environmental monitoring, underground infrastructure monitoring, sports field monitoring, border patrol control, and landslide protection. Monitoring and sensing in the subsoil are activities and deployments in the subsoil in order to collect necessary sensory data in the soil, store, and process to supply helpful information for applications relevant to the subsoil.

Sensor networks in the subsoil are deployed to monitor the temperature, volume water content (VWC), electrical conductivity [1], Soil pH and nutrient (nitrogen, phosphorus and potassium) [2], soil's manures [3], and Toxicity in soil [4]. Generally, sensors are buried in the soil to collect data and send it to the surface. Burying sensors with cables to send data to the surface is ineffective and expensive. Moreover, sensors with cables can obstruct agriculture and transportation activities on the surface, and these activities can damage these sensory devices.

Consequently, applying wireless sensors overcomes the inefficiency of wiring methods. Moreover, wireless sensors improve and ensure the flexibility and robustness of sensor networks in subsoil applications. In current sensory applications, the wireless sensor network has proven to have huge benefits in sensor applications. Among popular platforms for wireless sensor networks, LoRa is emerging as an efficient wireless system for low-cost sensor network applications. There are vast numbers of LoRa devices that allow deploying LoRa easily and quickly. Using LoRa is free. The frequencies of LoRa are in the ISM sub-GHz bands. Depending on the region, LoRa operates in the 433, 868 and 915 MHz bands [5]. LoRa is appropriate for low-power consumption applications. LoRa power varies from -4 dBm to 20 dBm, in 1 dB steps. Thus, if lower transmit powers are used, the consumption power of the LoRa device is rather low, and LoRa devices often have a lifetime of years.

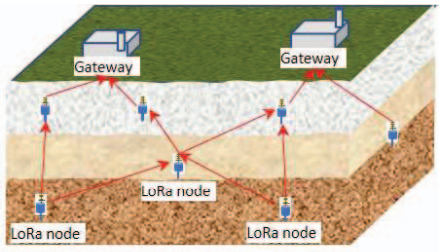

Fig. 1. Underground LoRa sensors network.

In this research, we focus on underground sensing and monitoring systems created by a network based on LoRa devices. A typical configuration of an underground wireless sensor network based on LoRa is depicted in Fig. 1. LoRa nodes which are integrated with sensors are buried in the subsoil layer. After collecting sensory data, LoRa nodes send signals to the gateways on the surface. LoRa nodes also can relay the signals so that deeper LoRa nodes can transfer signals efficiently to receivers on the surface.

Although exploiting LoRa devices to build underground sensor networks inherits some straightforward features of LoRa technology, wave propagation of LoRa devices in the soil is the biggest problem. High signal loss is always an unavoidable problem when signals propagate through the soil. Many studies present the extreme loss of signal propagating through the soil [6]–[8]. Soil consists of water, soluble minerals, and organic compounds. These soil substances generally

2325-2944/23/$31.00 ©2023 IEEE
DOI 10.1109/DCOSS-IoT58021.2023.00075

have high absorption rates on EM waves. Moreover, the soil has heterogeneous or layered structures. In addition, the soil can contain many unexpected objects such as tree roots, stones, rocks, and underground constructions. Therefore, the signal propagating through the soil severely suffers adverse radio wave propagation phenomena such as reflection, refraction, diffraction, and scattering [9]. These phenomena strongly reduce the signal's strength and severely deteriorate the signal's quality.

Signal propagation from the soil to the surface presents many challenges, making it necessary to evaluate propagation channels for underground wireless sensing and monitoring applications. Typically, a propagation channel is evaluated through either theoretical models or direct measurements. Using theoretical models can be cost-effective and save time when assessing the impact of the propagation medium on the propagating signal. However, theoretical models require many soil parameters that often lack accuracy. Building a theoretical model with a realistic soil structure can be complex and impractical, limiting the use of these models to simple soil structures and evaluations of signal loss only [6]. Consequently, the empirical evaluation of the EM wave propagation in the soil is an efficient and quick method when building underground sensor networks in the subsoil layers.

Numerous empirical studies have investigated signal propagation through the soil. However, most prior research has focused solely on calculating signal loss [10], [11], despite the fact that propagating signals are typically modulated to convey data. Currently, there is a lack of comprehensive evaluation of the relationships between modulation schemes and the efficiency and reliability of wireless communication links through inhomogeneous soil. Moreover, soil properties and ingredients vary across different locations and are susceptible to changes caused by weather conditions. Therefore, empirical evaluations of signal propagation through the soil require observing dynamic soil parameters at various times and positions to accurately reflect the soil's behaviour and effects on signal propagation.

Although the soil structures and ingredients are the main factors that affect signal propagation performance through the soil, analyzing the comprehensive soil structures and soil ingredients is complicated and difficult. However, not all the soil structures and ingredients directly and instantly affect the communication links. Among soil ingredients such as sand, clay, rock, water, and mineral, water is directly and frequently relevant to signal propagation performance. The quantity of water in the soil is characterized by the volume of water content (VWC) metric. Changing the water content in the soil can change the soil's electrical conductivity (EC). Both VWC and EC are simultaneously and directly related to signal attenuation. Therefore, we select these two parameters in evaluating signal propagation through the soil. Moreover, the measurement of VWC and EC is quick and straightforward by appropriate sensors. These sensory data can be used to calculate the propagation channel in practical applications.

In practical applications, besides selecting the proper parameters to evaluate the effects of soil conditions on signal propagation, the power supply problem is an additional challenge. The difficulty in installing and retrieving underground devices requires adequate power management to extend underground devices' lifetime. Moreover, power consumption is associated with signal types. Using highly reliable modulation schemes is one of the solutions for sending data in low-data-rate applications. However, these modulation schemes can cost higher power [12]. We realize that using appropriate modulation schemes for a communication link at different soil instant conditions can save energy and ensure the integrity of sensory data.

In this study, we aim to investigate the impact of modulation features on the dependability of wireless communication links between transmitters in soil and receivers on the soil surface. Specifically, we conduct empirical research to examine the influence of soil volume water content and soil electrical conductivity values on the reliability of these communication links. By exploring these factors, we can gain insights into improving the performance of wireless communication in soil environments, which has important practical implications for various fields such as agriculture and environmental monitoring.

In summary, our contributions are:

- thoroughly investigate the influences of LoRa modulation features such as bandwidth and spreading factor at different soil conditions on the received signal performance;
- proposes a reasonable, quick and efficient method to evaluate the effects of necessary soil's instant parameters on the performance of modulated signals;
- design and customize feasible LoRa transmitter and receiver that can be applied in practical sensing and monitoring application;
- implements an efficient protocol to control and synchronize between the buried transmitter and the receiver on the soil surface.

The following structure of our paper is organized as follows. Section II presents the recent relevant research to this article. We describe our experiment configuration in Section III. The results are illustrated in Section IV. Finally, Section V provides the conclusion.

II. Related work

Wireless communication in the soil can be conducted by the magnetic induction (MI) method or the electromagnetic wave propagation (EM) method [7]. Both methods are based on the electromagnetic field. MI is a communication technique whose communication links are established by the magnetic induction between two coils. In MI communication, coils are put near each other in terms of relative wavelength to ensure enough magnetic coupling between coils. Hence, MI methods usually operate at low frequencies from a few kilohertz to dozens of megahertz, [8], [13], [14].

The coupling between coils is related to permeability [15]. Therefore the MI communication link budget in the soil is

quite independent of the diversity of the soil. Nearly substances in the soil have the same permeability. Especially common soil substances such as water, clay, sand, and rock have the same permeability as free air. The paper of Akylyn suggested equipping small-size coils in sensing devices for underground communication [8]. Unfortunately, the applications of the MI method are quite limited. High loss is a striking problem when establishing communication links in the soil. MI coil coupling operates in the near field zone where the attenuation rate per distance is proportional to the power cubic of the distance between two well-aligned coils [8], [13], [14]. Moreover, the coil has a narrow generated magnetic flux pattern. This disadvantage feature makes aligning coils in the soil to be difficult and slow.

The other more popular wireless communication method is EM. There are abundant EM communication devices for sensing and monitoring applications in the air. The EM communication link is established by electromagnetic waves propagating from a transmitting antenna to a receiving antenna. EM antennas can offer a variety of radiation patterns according to the typical requirements in applications. Generally, Omnidirectional and wide-pattern antennas are popularly used in sensing and monitoring applications. Using these types of antennas assists in installing sensor nodes quicker and easier.

In recent years, the topics relevant to the propagation of EM waves through the soil in sensing and monitoring applications have attracted the attention of numerous scientists. Vuran et al., in [16], have mentioned in their paper that the phenomena such as multi-path, diffraction, scattering, and reflection can degrade the radio signal in their paper. However, analysing these effects on signal performance is sophisticated and inaccurate. Most theoretical models are currently built to calculate the path loss caused by some simple soil structure and attenuation coefficient. Notably, the authors evaluated the error rate under multi-path impact based on Rayleigh distribution, presented the effect of water volume on the path loss, and considered the reflection of the surface.

Concurrently with theoretical research, several empirical studies were conducted to evaluate the performance of signal propagating through the soil. The wireless sensor network experiments were performed by transmitting EM signals from a transmitter at a maximum depth of 45 cm [10] to a receiver at a distance of 100 cm. Nevertheless, these experiments were carried out to detect the relationships between signal loss and communication distance. In their experiments, the authors select the frequency of 433 MHz to measure. All these experiments are conducted in a small soil tank. Hence, the electromagnetic field distribution under the constraint boundary of the soil tank can differ from the electromagnetic field distribution caused by the extending boundary condition in natural soil. Moreover, these experiments were conducted to explore only the impacts of transmitter power on the received at different communication distances.

Similarly, the authors in [17] also conducted experiments to evaluate communication links through the soil. In these experiments, the authors buried the transmitter in the natural soil to transmit data packets by a signal modulated at 2.4 GHz. In this paper, the packet reception rate is the metric to evaluate the effects of the soil on the propagating signal. The authors measured the packet reception rate at different communication distances. However, in these experiments, the buried transmitter is not entirely isolated from the soil surface. The authors used a control and power cable to connect the buried device to a device on the surface. With this experiment setup, the leaky signals through the cable can create significant errors in experiment results.

Most wireless sensors based on popular wireless techniques such as LoRa, WiFi, and Bluetooth operate at frequencies from hundreds of megahertz to several gigahertz. Among these available wireless communication platforms, we suggest evaluating LoRa signals when propagating in the soil. The LoRa modulation technique is selected in our experiments because the high sensitivity characteristic of LoRa can overcome the high attenuation problem caused by soil. Moreover, the frequency band used by LoRa [18] and Chirp spectrum techniques are also advantageous for propagating EM signals in complex soil structures. The LoRa susceptibility to multipath propagation is also presented in [19]. The authors conducted experiments to evaluate the LoRa quality in a closed chamber whose walls can bounce the signal. Thus, the author can evaluate the multipath phenomenon in this chamber. The other study is conducted to investigate the reliability of LoRa in long-range applications [20]. These experiments were carried out to evaluate LoRa performance in many configurations, such as indoor, outdoor, and part of underground (in a shallow, open well near the surface).

In our experiments, the LoRa transceivers are customized to communicate with different LoRa modulation schemes at the frequency band of 866 MHZ. Also, we develop an algorithm to control and synchronize the packet sending between the buried transmitter and the receivers on the soil surface. During experiments, the LoRa packets are sent by the buried transmitter at different depths to the receivers laid on the surface at different distances. Besides deploying LoRa devices, we also deploy sensors to measure the VWC and EC of the soil near the test site. The cycles of measuring VWC and EC values are always synchronized with the cycles of sending LoRa packets.

The experiments with LoRa signal propagation through the soil are additionally found in the paper of [21]. Although the experiments were conducted with the LoRa signal propagation, the authors investigated the attenuation of only one type of LoRa modulation signal. The signal modulation features are not considered in this study. In the experiments, only antennas are buried in the soil. The LoRa transmitter and receiver are still on the surface so that the leaky signal can be strong enough to create errors. Since LoRa modulation specification [22] has a high sensitivity, the leaky signals can keep the high received packet rate. Thus, the communication link of 80 m in these experiments is mainly created by the leaky signals.

III. Experiment Method

A. Experiment setup in the soil

In this empirical study, we set up experiments in the test field to evaluate the signal sent from the soil to the surface. The LoRa devices are programmed to transmit a wide range of LoRa signal schemes by combining values of spreading factors, bandwidths and frequencies. Figure 2 describes the whole experiment process. A transmitter is buried into the soil at different depths from 0.3 m to 0.9 m. Five receivers are laid on the surface to receive the signal. We deploy these receivers at the same horizontal distance in every experiment to increase the accuracy of measurements. Then, the receivers measure the signal strength and decode the data. A data logger with an SD card is connected to these sensors to collect the sensory data during the experiments.

Near the position of the sensors, a cylindrical hole is dug into the soil to install the transmitter. Since the LoRa module has a relatively high sensitivity, we cover all buried devices by the soil and release the nearby soil surface to the original state to prevent any unnecessary leaky signal. The LoRa signal is transmitted to above-ground receivers at every transmitter's depth. Five identical receivers on the ground receive the signal simultaneously. Figure 2 presents the position of these receivers on the soil surface. The receivers' horizontal distance is measured from where we bury the transmitter. These receivers are shifted along a straight path with the distances of 1 m, 2 m, 5 m, 10 m, 15 m and 20 m.

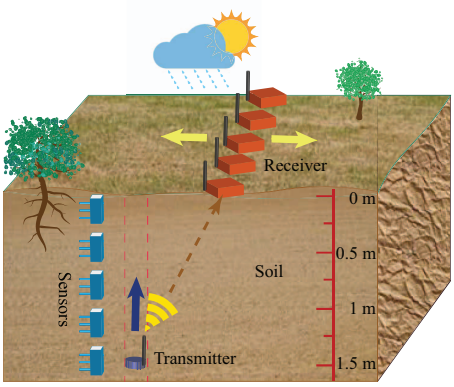

Fig. 2. Position of devices during experiments.

The LoRa transmitters are stored in highly waterproof plastic boxes to keep electronic circuits safe when buried in the soil, as in Figure 3. However, the antennas are waterproof, so they are mounted from the outside of the boxes to keep the alignment of the antennas straightforwardly. These antennas have linear polarization. When the boxes are buried in the soil for measurements with vertical polarization of antennas, the testing antennas are aligned perpendicular to the soil surface. With horizontal polarization experiments, the testing antennas are installed parallel to the soil surface to generate horizontally polarized waves. After digging the hole with a certain depth into the soil, we install the modules with the right antenna directions. Then we cover the transmitter modules and their antennas with the same soil on the testing side.

Fig. 3. Waterproof box.

The experiments are conducted on a public grassland of The Organic Gardening Drienerlo in The University of Twente Campus. According to [23], the soil in this test site mainly comprises sand and clay. In the layer near the surface, the soil is mixed with humus. There also exist some gravel and iron minerals in the deep position. We use METER's sensor TEROS 12 devices [24], which are frequently deployed in soil research and measurement because this sensor can measure the soil's volume water content and electrical conductivity with high accuracy [25]–[27].

B. Packet Control and Data Recording

In every measurement, the transmitter consecutively generates various LoRa signals, alternatively configured from seven spreading factors and three sizes of bandwidths. With every experiment configuration, we need to send about thirty-six different LoRa packets in the combinations of various LoRa settings. After a sending cycle, the transmitter has to stop and switch to sleep mode to save energy. Simultaneously, the transmitter and receivers are programmed to switch the data transmission mode to sleep mode for 30 minutes to save power.

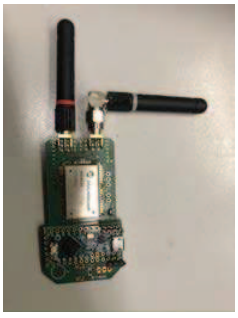

Fig. 4. LoRa module with two antennas.

Since the buried transmitter is electrically isolated from any device on the surface, we have to design a wireless packet control process to send and receive LoRa signals and save the power of LoRa transceivers. Each LoRa module is equipped with two antennas. One antenna is for controlling and the other for evaluating and testing, as shown in Fig. 4. While

the LoRa signal for evaluation is fixed at 863000005 Hz, the control frequency is selected at 433150000 Hz. Moreover, these antennas are perpendicularly mounted to each other to reduce interference between the control channel and other LoRa signals. These frequencies are unique to avoid interference with other popular frequencies around the band of 433 MHz and 866 MHz. Moreover, the control frequency and the frequency for evaluation are allocated in two apart frequency bands to eliminate any potential interference between the control frequency and the evaluated frequency.

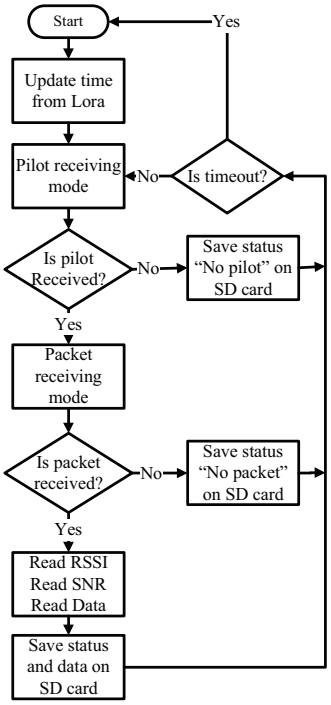

Fig. 5. Flowchart of packet control in the receiver.

The flowchart of power management and packet control is illustrated in Figure 5. When starting the experiments, the LoRa receivers and modules of VWC sensors update the real-time clock generated from a wireless clock generator that connects to the GPS real-time module. The real-time clock generator sends real-time clocks by the fixed LoRa signal at a frequency of 434700000 Hz, a bandwidth of 125 kHz, and a spreading factor of 12. After updating the real-time clock, the receivers switch to the pilot receiving mode to wait for the incoming control packet at the fixed LoRa setting with a frequency of 433150000 Hz, a bandwidth of 125 kHz, and a spreading factor of 12.

When the pilot packet comes, every receiver reads the LoRa pilot information. If the pilot fails, the receiver saves the status and switches to the pilot receiving mode again to wait for the next pilot. Otherwise, the receiver reads the information in the pilot packet about the next incoming data packet. After successfully receiving the pilot, the receiver switches to receiving data packet status with the new bandwidth and new spreading factor informed by the previous pilot packet. When the data packet is successfully received, the receiver measures the RSSI and decodes the data attached to the data packet's payload. After decoding the data, the receiver writes the decoded data and RSSI value to the attached SD card. Then, the receivers switch to the pilot receiving mode and wait for the next pilot. If the receiver cannot decode the data in the payload, it saves the status, switches to the pilot receiving mode, and waits for the next pilot.

The timing and synchronization of LoRa packets during experiments are depicted in Figure 6. After the receiver updates the real-time information, the microcontroller sends commands requesting the LoRa chip switch to pilot receiving mode. Next, the receivers receive and read the pilot's information. Based on the information received from the pilot packet, the receiver switch to the packet-receiving mode. After sending a pilot packet, the transmitter prepares to send the following data packet. Sending data packets is always delayed about one minute after the receive wakes up to ensure the receiver has enough safe time to switch to receive packets.

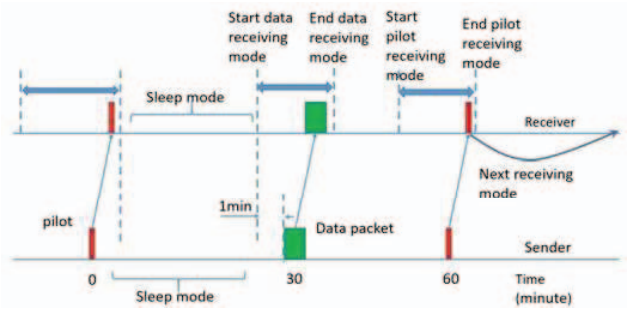

Fig. 6. Timing of pilot packets and data packets.

When the pilot or the data packet cannot reach the receiver, the pilot receiving mode and packet receiving mode always have specific timeouts before the receivers are forced to the pilot receiving mode. Figure 7 explains how the receiver keeps receiving the data when there are some errors. If the pilot or data packet fails, the receiver is always scheduled to switch to pilot receiving mode again and wait until the next pilot is successfully received.

The transmitter has a microcontroller, a LoRA circuit RN2483 and a micro SD card. The microcontroller controls transmitting and timing sessions during the measurements and stores recorded data on the SD cards. The modules are buried for several days during experiments. Then, we dig the modules out, retrieve the data from the SD card and recharge the battery for the next experiments. Thus, with this algorithm for packet timing and controlling, we can bury a transmitter powered by a lithium-ion battery of 3.7 V and 12000 mA to transmit 36 LoRa packets per 30 minutes. The transmitter can operate for at least a month before being retrieved to recharge the batteries.

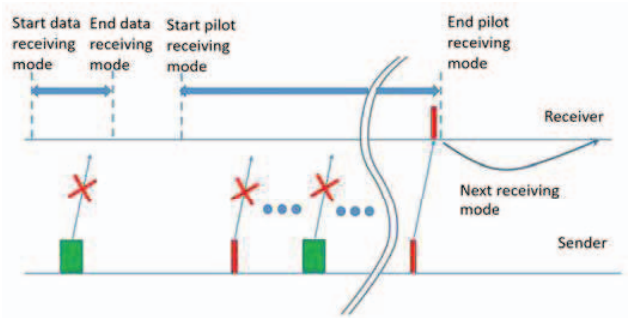

Fig. 7. Packet failing control.

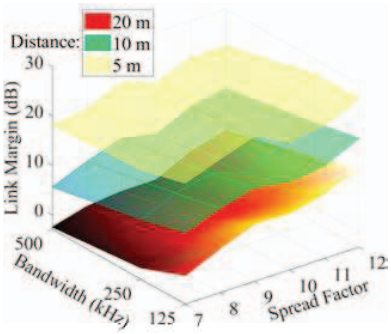

Fig. 8. Link margin results at the depth of 0,7 m, vertical polarization

IV. Experiment Results

TABLE I
Sensitivity according to the LoRa settings (dBm) of SX1276 LoRa chip [28]

BW	SF	7	8	9	10	11	12
125	[kHz]	−123	−126	−129	−132	−133	−136
250	[kHz]	−120	−123	−125	−128	−130	−133
500	[kHz]	−116	−119	−122	−125	−128	−130

After receiving the value of RSSI of a data packet, we calculate the link margin based on the typical sensitivity in Table I. Finally, we receive the link margins of every LoRa setting at different distances, depths, antenna directions, and soil conditions. The link margins vary according to distance, depth and polarization. We present the experiment results with the wet soil condition in the following subsections: A, B and C. The link margins in dry and wet soil are compared in subsection D. The experiments are conducted for several months to meet the wet and dry soil conditions. The dry soil experiments are conducted during July when there is less rain.

A. Effects of Different Distances

With every position of the buried transmitter, we move the receivers at different distances on the surface.. The experiment results in wet soil are illustrated in Figure 8. The graphs in Figure 8 explains the experimental setup with a typical transmitter depth of $0.7\,\mathrm{m}$. The receivers measure RSSIs to evaluate the link margin of the modulation schemes of signals. In general, the signal attenuation increases with the distance. However, the proper selection of LoRa settings can produce a higher link margin. Figure 8 presents the link margins at the distances of $5\,\mathrm{m}$, $10\,\mathrm{m}$, and $20\,\mathrm{m}$ at a typical depth of $0.7\,\mathrm{meter}$. The wet soil's parameters are listed in Table II. The increase of the loss with the distance is nonlinear. Besides the free-space path loss, the loss is also included in the other non-predicted losses. In general, the loss varies when the receivers' distance changes. Typically, the loss increases from 5 dB when the communication range changes from 5 m to 10 m. When we move receivers from 10 m to 20 m, the loss increases 10 dB.

These experiment results allow explaining the effects of LoRa modulation features on the reliability of communication links. The experiment results are illustrated in Figure 8. In this figure, the LoRa signals with narrow bandwidths and high spreading factors offer high link margins. Among LoRa settings, the LoRa signal with a wider bandwidth of 125 kHz and a spreading factor of 7 usually produces the highest link margin. The sensitivity value in Table I, which is higher for lower bandwidths and smaller spreading factors, explains the increase of the link margin. At the distance of 20 m, the attenuation is high. The wide-bandwidth and low-spread-factor LoRa signals can cause the link margin to drop below 0 dB. The decoding error rate frequently occurs with LoRa settings that produce negative link margins. Typically, at the receiver distance of 20 m and transmitter depth of $0.7\,\mathrm{m}$, the LoRa setting with a bandwidth of 500 kHz and spreading factor of 7 produces a link margin of -2.5 dB. Meanwhile, the signal with a narrow bandwidth of 125 kHz and spreading factor 12 produces 12.95 dB of link margin.

TABLE II
Volume Water Content (VWC) and Electrical Conductivity (EC) with Resolution $0.001\,\mathrm{m}^3/\mathrm{m}^3$ of TEROS 12 Sensor

Sensors Depth	Wet Soil Conditions	
	VWC	EC
$0.5\,\mathrm{m}$	$0.223\,\mathrm{m}^3/\mathrm{m}^3$	$0.031\,\mathrm{dS/m}$
$0.7\,\mathrm{m}$	$0.288\,\mathrm{m}^3/\mathrm{m}^3$	$0.088\,\mathrm{dS/m}$
$0.9\,\mathrm{m}$	$0.307\,\mathrm{m}^3/\mathrm{m}^3$	$0.151\,\mathrm{dS/m}$

B. Effects of Different Depths

The previous subsection presents the results of experiments at a fixed depth and different receiver distances. In the following experiments, we evaluate the effects of LoRa settings on the link margin at different depths while the receiver is laid at a fixed distance on the soil surface. The experiment setup with the receivers' distance of $10\,\mathrm{m}$. The transmitter is buried at depths from 0.3 m to 1.5 m. Figure 9 presents typical results of link margins of the depths of $0.5\,\mathrm{m}$, $0.7\,\mathrm{m}$, and $0.9\,\mathrm{m}$. The experiments are conducted at the soil conditions listed in Table II.

The experiment results show that depth strongly causes signal loss. At the receiver distance of $10\,\mathrm{m}$ on the soil surface, when the transmitter depth increases $0.2\,\mathrm{m}$ from $0.5\,\mathrm{m}$ to

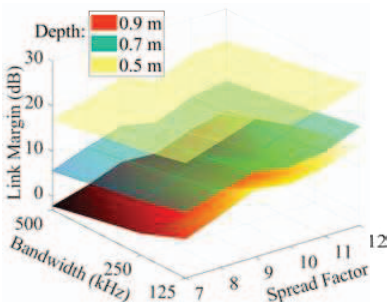

Fig. 9. Link margin with different depths at distnace of 10 m, vertical polarization

0.7 m and from 0.7 m to 0.9 m, the communication distance between transmitter and receiver is nearly unchanged. However, the loss increases significantly with this depth increment. The results of the loss vary with different depths. When the transmitter's depth changes from 0.5 m to 0.7 m, the loss increases approximately 6 dB. Whereas the loss increases approximately 10 dB when the transmitter is moved from 0.7 m to 0.9 m below the surface.

Therefore, these loss differences are almost relevant to the water in the soil and the electrical conductivity of the soil. According to Table II, the electrical conductivity increases more dramatically than the volume of water content does. Since the soil ingredients are not uniform, the soil near the surface has an electrical conductivity of 0.031 dS/m at 0.5 m. This electrical conductivity increases to 0.088 dS/m at 0.7 m and to 0.151 dS/m at 0.9 m. Meanwhile, the VWCs at these depths are similar. At the depths of 0.5 m, 0.7 m, and 0.9 m, VWCs are respectively $0.223\,\mathrm{m}^3/\mathrm{m}^3$,$0.288\,\mathrm{m}^3/\mathrm{m}^3$, $0.3078\,\mathrm{m}^3/\mathrm{m}^3$.

When the transmitter is buried at a depth of 0.9 m and the receivers are placed at a distance of 10 m, the signal suffers relatively high attenuation. This high loss is mainly caused by the high electrical conductivity of the soil and the soil's heterogeneity. With a LoRa signal at a bandwidth of 500 kHz and a spreading factor of 7, the link margin is -2.19 dB. In comparison, the link margin in this experiment setup increases to 15.23 dB with a bandwidth of 125 kHz and a spreading factor of 12.

Similar to the results of the previous experiments, the proper LoRa setting can improve the link margin. According to Table I, half the size of the bandwidth or an increment step of the spreading factor can contribute approximately to a link margin of 3 dB. By theory calculating, the difference between the highest and lowest link margin is 21 dB. In reality, the differences between the highest and lowest link margin are 18.14 dB, 13.414, and 10.96 db at the depths of 0.9 m, 0.7 m, and 0.5 m.

C. Effects of Antenna Polarization

Depending on the vector electric field's polarization, the effects on signal propagation through the soil are different because the soil structures are not uniform, and the propagation path goes through the soil surface. The polarization of the electric field is relevant to the form of the antenna. Most simple antennas generate only the linear polarization electric field. The linear polarization has the generated E field vectors, which are always parallel during transmission. Generally, dipole or monopole antennas are preferred in sensor applications because these antennas are cheap. The electric field of these antennas usually is parallel to these antennas. Thus, according to the antenna's direction to the soil surface, these antennas can generate vertical or horizontal polarization. The results in Figure 10 show that horizontal polarization usually suffers higher loss than vertical polarization.

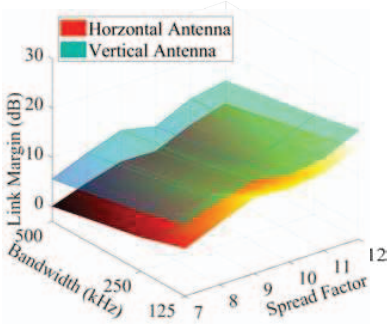

Fig. 10. Link margin of antenna polarization, depth of 0.7 m and distance of 10 m, vertical polarization.

D. Effects of Soil Conditions

Since soil conditions change according to the weather, conducting experiments at different months is necessary to compare the various influences of dry and wet soil. Figure 11 depicts the multiple effects of LoRa settings in dry and wet soil. The typical experiments setup with the transmitter's depth of 0.9 m and the receivers' distance of 10 m. These results are from the experiments of the driest and wettest soil conditions. The VWCs and ECs in the dry and wet conditions are listed in Table III.

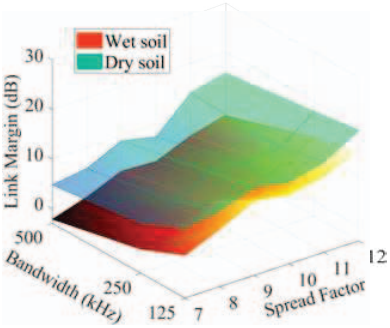

Fig. 11. Link margin under influences of humidity, distance of 20 m, depth of 0.9 m.

Figure 11 presents the differences in link margin results between soil conditions. Usually, the signal suffers higher loss in wet conditions than in dry soil. The link margin values

measured in the dry soil are always higher than the link margin values measured in the wet soil. The differences in link margins between two soil conditions vary from 6 dB to 12 dB among LoRa settings.

TABLE III
VOLUME WATER CONTENT AND ELECTRICAL CONDUCTIVITY OF WET AND DRY SOIL

Sensor's Depth	Soil Conditions			
	Dry soil		Wet soil	
	VWC (m^3/m^3)	EC (dS/m)	VWC (m^3/m^3)	EC (dS/m)
0.5 m	0.059641	0.000	0.223094	0.031
0.7 m	0.205901	0.064	0.287854	0.088
0.9 m	0.261572	0.031	0.307187	0.151

In the dry soil conditions, all link margins of all LoRa settings in these experiments are higher than 5 dB. According to Fig. 11, the LoRa with a bandwidth of 500 kHz and a spreading factor of 7 has a negative link margin of -2.19 dB. At this negative link margin. Meanwhile, with the same LoRa setting, in the dry condition, the link margin is 4.75 dB.

V. CONCLUSION

The experiment results show that the depth and electrical conductivity affect the LoRa signal's link margin. With the reasonable packet cycle and power management, deploying a wireless sensing network with the LoRa modulation in the subsoil is promising and applicable. With highly reliable LoRa devices, the LoRa modulation technique is also a cheap and quick solution for wireless sensing applications in the subsoil. Vertical antennas can offer higher reliability and eliminate the complexity of aligning antennas.

REFERENCES

[1] Chen, Yong, Gary W. Marek, Thomas H. Marek, Kevin R. Heflin, Dana O. Porter, Jerry E. Moorhead, and David K. Brauer. "Soil water sensor performance and corrections with multiple installation orientations and depths under three agricultural irrigation treatments." Sensors 19, no. 13 (2019): 2872.

[2] Chen, Yong, Gary W. Marek, Thomas H. Marek, Kevin R. Heflin, Dana O. Porter, Jerry E. Moorhead, and David K. Brauer. "Soil water sensor performance and corrections with multiple installation orientations and depths under three agricultural irrigation treatments." Sensors 19, no. 13 (2019): 2872.

[3] Rigby, Dan, and Daniel Cáceres. "Organic farming and the sustainability of agricultural systems." Agricultural systems 68, no. 1 (2001): 21-40.

[4] Odukkathil, Greeshma, and Namasivayam Vasudevan. "Toxicity and bioremediation of pesticides in agricultural soil." Reviews in Environmental Science and Bio/Technology 12 (2013): 421-444..

[5] Jebril, Akram H., Aduwati Sali, Alyani Ismail, and Mohd Fadlee A. Rasid. "Overcoming limitations of LoRa physical layer in image transmission." Sensors 18, no. 10 (2018): 3257.

[6] Akyildiz, Ian F., and Erich P. Stuntebeck. "Wireless underground sensor networks: Research challenges." Ad Hoc Networks 4, no. 6 (2006): 669-686.

[7] Akyildiz, Ian F., Zhi Sun, and Mehmet C. Vuran. "Signal propagation techniques for wireless underground communication networks." Physical Communication 2, no. 3 (2009): 167-183.

[8] Sun, Zhi, and Ian F. Akyildiz. "Underground wireless communication using magnetic induction." In 2009 IEEE International Conference on Communications, pp. 1-5. IEEE, 2009.

[9] Balanis, Constantine A. Antenna theory: analysis and design. John Wiley & Sons, 2015.

[10] Silva, Agnelo R., and Mehmet C. Vuran. "Empirical evaluation of wireless underground-to-underground communication in wireless underground sensor networks." In Distributed Computing in Sensor Systems: 5th IEEE International Conference, DCOSS 2009, Marina del Rey, CA, USA, June 8-10, 2009. Proceedings 5, pp. 231-244. Springer Berlin Heidelberg, 2009.

[11] Xiaoya, Hu, Gao Chao, Wang Bingwen, and Xiong Wei. "Channel modeling for wireless underground sensor networks." In 2011 IEEE 35th Annual Computer Software and Applications Conference Workshops, pp. 249-254. IEEE, 2011.

[12] Bouguera, Taoufik, Jean-François Diouris, Jean-Jacques Chaillout, Randa Jaouadi, and Guillaume Andrieux. "Energy consumption model for sensor nodes based on LoRa and LoRaWAN." Sensors 18, no. 7 (2018): 2104.

[13] Shamonina, Ekaterina, V. A. Kalinin, K. H. Ringhofer, and Lazlo Solymar. "Magnetoinductive waves in one, two, and three dimensions." Journal of Applied Physics 92, no. 10 (2002): 6252-6261.

[14] Syms, R. R. A., E. Shamonina, and L. Solymar. "Magneto-inductive waveguide devices." IEE Proceedings-Microwaves, Antennas and Propagation 153, no. 2 (2006): 111-121.

[15] Rose, James H., Erol Uzal, and John C. Moulder. "Magnetic permeability and eddy-current measurements." Review of progress in quantitative nondestructive evaluation 14 (1995): 315-315.

[16] Vuran, M. Can, and Agnelo R. Silva. "Communication through soil in wireless underground sensor networks–theory and practice." Sensor Networks: Where Theory Meets Practice (2009): 309-347.

[17] Stuntebeck, Erich P., Dario Pompili, and Tommaso Melodia. "Wireless underground sensor networks using commodity terrestrial motes." In 2006 2nd IEEE Workshop on Wireless Mesh Networks, pp. 112-114. IEEE, 2006.

[18] Devalal, Shilpa, and A. Karthikeyan. "LoRa technology-an overview." In 2018 second international conference on electronics, communication and aerospace technology (ICECA), pp. 284-290. IEEE, 2018.

[19] Staniec, Kamil, and Michał Kowal. "LoRa performance under variable interference and heavy-multipath conditions." Wireless communications and mobile computing 2018 (2018).

[20] Cattani, Marco, Carlo Alberto Boano, and Kay Römer. "An experimental evaluation of the reliability of lora long-range low-power wireless communication." Journal of Sensor and Actuator Networks 6, no. 2 (2017): 7.

[21] Wan, Xue-fen, Yi Yang, Jian Cui, and Muhammad Sohail Sardar. "Lora propagation testing in soil for wireless underground sensor networks." In 2017 Sixth Asia-Pacific Conference on Antennas and Propagation (APCAP), pp. 1-3. IEEE, 2017.

[22] Ertürk, Mehmet Ali, Muhammed Ali Aydın, Muhammet Talha Büyükakkaşlar, and Hayrettin Evirgen. "A survey on LoRaWAN architecture, protocol and technologies." Future Internet 11, no. 10 (2019): 216.

[23] Dente, Laura, Z. Vekerdy, Z. Su, and Murat Ucer. Twente soil moisture and soil temperature monitoring network. University of Twente, 2011.

[24] Mokari, Esmaiil, and Manoj K. Shukla. "Field Evaluation of TEROS 12 Sensor for Estimating Saturated Extract EC in a Clay Soil." In AGU Fall Meeting Abstracts, vol. 2019, pp. H53N-1980. 2019.

[25] Chen, Yong, Gary W. Marek, Thomas H. Marek, Kevin R. Heflin, Dana O. Porter, Jerry E. Moorhead, and David K. Brauer. "Soil water sensor performance and corrections with multiple installation orientations and depths under three agricultural irrigation treatments." Sensors 19, no. 13 (2019): 2872.

[26] Goswami, Manash Protim, Babak Montazer, and Utpal Sarma. "Design and characterization of a fringing field capacitive soil moisture sensor." IEEE transactions on instrumentation and measurement 68, no. 3 (2018): 913-922.

[27] Singh, Jasreman, Derek M. Heeren, Daran R. Rudnick, Wayne E. Woldt, Geng Bai, Yufeng Ge, and Joe D. Luck. "Soil structure and texture effects on the precision of soil water content measurements with a capacitance-based electromagnetic sensor." Transactions of the ASABE 63, no. 1 (2020): 141-152.

[28] Augustin, Aloÿs et al. "A Study of LoRa: Long Range and Low Power Networks for the Internet of Things." Sensors (Basel, Switzerland) vol. 16,9 1466. 9 Sep. 2016, doi:10.3390/s16091466